Physical characteristics of collimators for dual-isotope imaging with Tc-99m and I-123

Tunninen, Virpi

SPRINGER-VERLAG SINGAPORE PTE LTD
2018

Tunninen , V , Kauppinen , T & Eskola , H 2018 , Physical characteristics of collimators for dual-isotope imaging with Tc-99m and I-123 . in H Eskola , O Väisänen , J Viik & J Hyttinen (eds) , EMBEC & NBC 2017 . IFMBE Proceedings , vol. 65 , SPRINGER-VERLAG SINGAPORE PTE LTD , Singapore , pp. 245-249 , Joint Conference of the European Medical and Biological Engineering Conference (EMBEC) / Nordic-Baltic Conference on Biomedical Engineering and Medical Physics (NBC) , Tampere , Finland , 01/06/2017 . https://doi.org/10.1007/978-9

http://hdl.handle.net/10138/327120
https://doi.org/10.1007/978-981-10-5122-7_62

acceptedVersion

Physical characteristics of collimators for dual-isotope imaging with ^{99m}Tc and ^{123}I

V. Tunninen[1], T. Kauppinen[2] and H. Eskola[3,4]

[1]Satakunta Central Hospital/Department of Nuclear Medicine, Pori, Finland
[2]Helsinki University Hospital/HUS Medical Imaging Center, Helsinki, Finland
[3]Faculty of Biomedical Sciences and Engineering, Tampere University of Technology, Tampere, Finland
[4]Department of Radiology, Tampere University Hospital, Tampere, Finland

Abstract—**The purpose of this study was to compare the physical characteristics of Low Energy High Resolution (LEHR), Low Energy Ultra High Resolution (LEUHR) and Medium Energy Low Penetration (MELP) collimators for simultaneous ^{99m}Tc and ^{123}I imaging. MELP collimator performed well with ^{123}I high-energy gamma photons, but low resolution makes it unsuitable to use for acquisition of small structures such as parathyroid adenomas. LEUHR collimators optimized for ^{99m}Tc have highest resolution, but the differences in septal penetration and sensitivity in favor of LEHR collimator needs to be tested with specific parathyroid phantoms.**

Keywords—**dual-isotope, ^{99m}Tc, ^{123}I, collimator, SPECT/CT.**

I. Introduction

Modern SPECT/CT is a standard clinical tool for various nuclear medicine procedures. Clinical work is usually performed with one radiopharmaceutical, but there are some applications using simultaneous dual-isotope imaging such as parathyroid scintigraphy with ^{123}I and ^{99m}Tc-sestamibi. Simultaneous use of ^{99m}Tc and ^{123}I is particularly challenging because of the close proximity of the photon energies (140keV and 158keV) and with limited energy resolution of a gamma camera.

Collimator selection for dual-isotope applications is always a compromise in terms of resolution, sensitivity and septal penetration of photons. It has been shown previously that "*the physical characteristics for ^{123}I imaging and dual-isotope imaging differ even between low energy collimators that provide similar sensitivity and spatial resolution*" [1].

The use of medium energy (ME) collimators reduces the influence of septal penetration of high-energy gamma photons of ^{123}I. However, ME collimators generally provide lower spatial resolution compared to that of low energy (LE) collimator, which may influence the detection of small structures such as parathyroid adenomas [1,2]. If the LE collimator is used to acquire good quality ^{99m}Tc images, the septal penetration of ^{123}I photons may be elevated and image contrast will be degraded [3]. The energy window selection, the contamination of one radionuclide photon into the energy window of the other (cross contamination), energy-dependent uniformity and sensitivity also need to be examined [4].

Several approaches are suggested for simultaneous ^{123}I/^{99m}Tc-imaging, e.g.:

1. Using narrow or asymmetric energy windows [5,6]
2. Using a subtraction method based on a single crossover factor [7]
3. Using a scatter correction method (TEW) [8]
4. Using complex and time-consuming model-based correction methods [9].

The septal penetration of high-energy photons of ^{123}I is also a potential cause of artefacts. It also effects on ^{123}I sensitivity as a function of distance, as high-energy photons penetrate through the lead into the crystal and behave as camera would be without collimator [2]. That is why suggested the physical characteristics should be investigated for each camera-collimator system used for dual-isotope imaging [1,3].

The aim of this study was to compare the physical characteristics of Low Energy High Resolution (LEHR), Low Energy Ultra High Resolution (LEUHR) and Medium Energy Low Penetration (MELP) collimators for ^{99m}Tc and ^{123}I imaging.

II. Materials and Methods

A Siemens Symbia Intevo T2 SPECT/CT (Siemens, Erlangen, Germany) in the Department of Nuclear Medicine of Satakunta Central Hospital was used in this study. All measurements were performed with three sets of collimators: LEHR, LEUHR and MELP (Table 1).

Table 1 Collimator specifications according to manufacturer

Collimator	MELP	LEHR	LEUHR
Hole length (mm)	40,64	24,05	35,8
Septal thickness (mm)	1,14	0,16	0,13
Hole Diameter (mm)	2,94	1,11	1,16
Sensitivity @ 10 cm (cpm/μCi)	275	202	100
System resolution @ 10 cm (mm)	12,5	7,5	6,0

Intrinsic uniformity was measured separately with ^{99m}Tc and ^{123}I according to the quality control routine by Siemens. ^{99m}Tc was measured using 140 keV 10% energy window and ^{123}I was measured using symmetric (158 keV, 10%) and asymmetric (167keV, 10%) energy windows. 60 million counts were collected for each measurement.

System sensitivity was measured for each collimator following the NEMA guidelines [10], using a 100mm plastic dish into which calibrated activity of (about 37MBq) each isotope (^{99m}Tc or ^{123}I) was instilled. Measurements were performed separately for each isotope using the above-mentioned energy windows with 10 cm distance from the collimator surface. Sensitivity was calculated as cpm/µCi.

System spatial resolution was measured in air with ^{99m}Tc and ^{123}I separately for each collimator following the NEMA guidelines [10]. A tube of 1mm inner diameter was filled with ^{99m}Tc or ^{123}I solution and placed at various distances from detector surface (0 cm, 10cm, 20 cm, 30cm, and 40 cm) parallel to the x axis of the camera using non-scattering material as a spacer. Images were collected on a 1024x1024 matrix with above-mentioned energy window settings.

SPECT spatial resolution and uniformity with scatter were measured with Jaszczak phantom with hot spot insert (Data Spectrum Corporation, Durham, North Carolina). The phantom was filled with 1,5GBq of ^{99m}Tc and acquired with clinical SPECT/CT acquisition protocol for all collimators (a noncircular orbit, 180° detector configuration, 128×128 matrix; 140 keV 10%, step-and-shoot, 48 views for each detector, 33 s/projection).

The CT acquisition was acquired after the SPECT acquisition without moving the phantom and using the same scan area as for SPECT (130 kVp, 2×2.5 mm collimation, 0.8 s rotation time, 1.5 pitch, CARE Dose AEC+DOM, with the ref. exposure 80 mAs). ^{99m}Tc images (with attenuation correction) were reconstructed on the Siemens Syngo workstation using the FLASH 3D-algorithm with four different parameter settings (6, 8, 16 or 32 iterations, 8 subsets, Gaussian 9.00 filter, with TEW scatter correction).

SPECT spatial resolution was evaluated visually, according to the visibility of the hollow channels (12,7mm (1), 11,1mm (2), 9,5mm (3), 7,9mm (4), 6,4mm (5) and 4,8mm (6)). To evaluate uniformity, a large circular ROI was drawn in uniform part of the phantom. The percent root mean square noise (%RMS) was calculated using the formula:

$$\%rms = \frac{SD}{mean} \times 100\% \qquad [1]$$

Spectrum for both isotopes was measured in air and with scatter separately for each collimator at various distances (10cm, 20cm, 30cm and 40cm). Measurements were repeated also with scatter (5cm water as scattering material) between the source and the detector.

Scatter-to-photopeak –ratio was measured using ^{99m}Tc and ^{123}I point sources of equal activity (80MBq) in air separately for each collimator at various distances (10cm, 20cm, 30cm and 40cm). Photopeak and scatter windows were set to 20% (photopeak and scatter windows being equal width in keV). Acquisition time per frame for each collimator was selected to avoid pixel overflow in any measurement. Uniformity correction was set off to avoid any adjustment of counts. Background counts were subtracted. Measurements were repeated also with scatter (5cm water as scattering material) between the source and the detector.

Cross-contamination was measured using two identical 1000 ml bottles filled with ^{99m}Tc and ^{123}I (~40MBq of each). A SPECT acquisition was performed with each bottle using previously mentioned acquisition protocol with both energy window settings and for all collimators. The cross-contamination was expressed as percentage of ^{99m}Tc counts in ^{123}I window of ^{99m}Tc counts in ^{99m}Tc window. The ^{123}I cross-contamination in ^{99m}Tc window was calculated in a similar manner.

III. Results

Integral uniformity at the useful field of view (UFOV) with symmetric energy windows were 3,1% and 2,2% with ^{99m}Tc and ^{123}I, respectively. With asymmetric ^{123}I energy window the uniformity was 11,9%.

System sensitivity with ^{99m}Tc was well in line with specifications given by Siemens. Sensitivity with ^{123}I symmetric energy window was higher with low-energy collimators compared to sensitivity with ^{99m}Tc, which is caused by septal penetration of high-energy gamma photons of ^{123}I. Asymmetric energy window with ^{123}I reduced sensitivity 15,0%-43,2% compared to symmetric energy window. System sensitivity results are presented in Table 2.

Table 2 System sensitivity for LEHR, LEUHR and MELP collimators measured with ^{99m}Tc and ^{123}I using symmetric and asymmetric energy windows.

Collimator	^{99m}Tc (cpm/µCi)	^{123}I symmetric (cpm/µCi)	^{123}I asymmetric (cpm/µCi)
MELP	220	205	117
LEHR	159	282	231
LEUHR	72	149	127

Measured FWHM for was similar for ^{99m}Tc and ^{123}I. For MELP collimator there was no difference in FWTM values for ^{99m}Tc and ^{123}I. For LE collimators, FWTM was larger with ^{123}I than that with ^{99m}Tc. There was no difference with symmetric and asymmetric energy windows for ^{123}I. The results are presented in Table 3.

Table 3 System spatial resolution at 20cm for LEHR, LEUHR and MELP collimators measured with ^{99m}Tc and ^{123}I using symmetric and asymmetric energy windows.

Collimator	FWHM (mm)		FWTM (mm)	
	^{99m}Tc	^{123}I	^{99m}Tc	^{123}I
MELP	17,3	16,8	30,0	29,9
LEHR	11,3	11,5	20,1	23,0
LEUHR	8,3	7,6	14,8	16,0

SPECT spatial resolution with MELP collimators was inadequate for acquisition of small structures. Only two largest channels could be identified. LEHR and LEUHR collimators performed better, as channels in sectors 3 and 4 could be identified, respectively. SPECT uniformity decreased with increasing resolution and number of iterations. The results are presented in Table 4.

Table 4 SPECT resolution and uniformity for LEHR, LEUHR and MELP collimators measured with ^{99m}Tc and ^{123}I using symmetric and asymmetric energy windows.

		Iterations			
		6	8	16	32
MELP	Resolution	1	1	2	2
	Uniformity (%rms)	3	3,3	4,2	5,9
LEHR	Resolution	3	3	3	3
	Uniformity (%rms)	3,1	3,4	4,4	5,6
LEUHR	Resolution	4	4	4	4
	Uniformity (%rms)	3,5	3,9	5,1	6,2

The shape of the spectrum in air for ^{99m}Tc was similar for all collimators and distances. Scattering material increased the amount of scatter, but there was no change in the shape as a function of distance or between collimators. Spectrum for ^{123}I in air was different for collimators (Figure 1) and also varied as a function of distance (Figure 2).

Scatter to photopeak –ratio in air with ^{99m}Tc was 13,0%-14,7% for all collimators and distances. With scatter, the ratio increased to 46,8%-49,3%. Distance between the source and collimator surface did not have any significant effect. Scatter to photopeak –ratio with ^{123}I was very different for all collimators and also as a function of distance (Table 5).

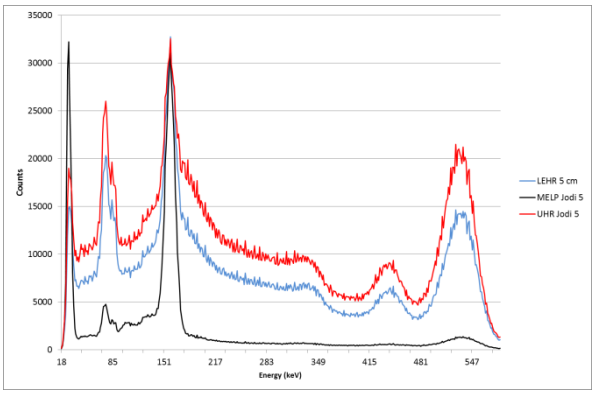

Figure 1. Spectrum of ^{123}I at 5 cm from detector in air for LEHR (blue), LEUHR (red) and MELP (black) collimators.

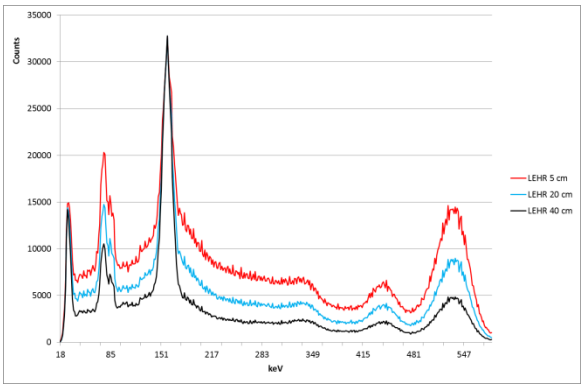

Figure 2. Spectrum of ^{123}I with LEHR collimator at 5 cm (red), 20cm (blue) and 40cm (black) from detector.

Table 5. Scatter to photopeak –ratio with ^{123}I for collimators in air and with scatter with 10cm, 20cm, 30cm, and 40 cm distance between source and collimator surface.

Collimator	10cm	20cm	30cm	40cm
MELP, air	20,0	18,9	17,9	16,7
MELP, scatter	58,1	57,5	57,2	57,0
LEHR, air	42,1	35,4	30,6	26,6
LEHR, scatter	57,9	54,7	52,0	50,2
UHR, air	53,4	47,0	41,7	36,7
UHR, scatter	67,0	64,5	62,5	60,9

Cross-contamination measurements showed similar contamination of ^{99m}Tc in ^{123}I window for all collimators. Asymmetric energy window for ^{123}I was reduced to approximately half when using asymmetrical energy window. ^{123}I contamination in ^{99m}Tc window was highest with LEUHR collimator and lowest with MELP collimator (Table 6).

Table 6 Cross-contamination of ^{99m}Tc and ^{123}I.

	^{99m}Tc-contamination in		^{123}I contamination in
	^{123}I symmetric	^{123}I asymmetric	^{99m}Tc
MELP	4,7 %	1,8 %	28,3 %
LEHR	4,7 %	2,0 %	40,7 %
LEUHR	5,1 %	2,6 %	50,6 %

IV. Discussion

The advantages of dual isotope method with ^{99m}Tc-sestamibi and ^{123}I for parathyroid scintigraphy have been acknowledged in several studies and is also recommended in the European Association of Nuclear Medicine (EANM) guideline for parathyroid scintigraphy [11]. Unfortunately dual isotope imaging with ^{99m}Tc and ^{123}I is a challenging task. Collimators optimized for ^{99m}Tc have problems with ^{123}I high energy photon septal penetration. ME collimators have less septal penetration, but the resolution is inadequate for detecting small structures as shown in this study.

SPECT acquisitions are performed with elliptical orbit in order to gain highest resolution possible. However, as shown in this study, both sensitivity and cross contamination of ^{123}I into ^{99m}Tc window are dependent on the distance between the source and the collimator which degrades the quantitative precision. Cross contamination of ^{99m}Tc into ^{123}I window is low. Although the injected activity of ^{123}I in clinical study is much lower than the activity of the ^{99m}Tc-sestamibi, the uptake of iodine in the thyroid gland is higher. The average activities of ^{123}I and ^{99m}Tc in the thyroid gland are thus comparable and the contamination of ^{99m}Tc in ^{123}I image is not significant. Shifting the ^{123}I window to the right decreases the amount of cross contamination and allows for wider scatter window between ^{99m}Tc and ^{123}I photopeak but in the expense of uniformity. The contamination of ^{123}I in ^{99m}Tc image is much higher regardless of the collimator. Shifting the ^{99m}Tc window to the left was not tested here, as being shown inappropriate previously [2].

The most important information in parathyroid scintigraphy is in the ^{99m}Tc-sestamibi image. The ^{123}I image is mainly used for removal of the thyroid gland. Although ^{99m}Tc image is contaminated with ^{123}I photons, their spatial distribution is different as parathyroid glands are separated from thyroid glands (excluding rare cases of intrathyroidal parathyroid glands). High resolution images are thus of high importance.

The choice of the collimator for simultaneous dual-isotope imaging is a compromise. LEUHR collimator has highest spatial resolution, but due to thinner septa the ^{123}I contamination in ^{99m}Tc image is higher. LEHR collimators has twice the sensitivity but in the expense of resolution. The suitability of both LE collimators for parathyroid imaging needs to be tested with specific phantoms in order to resolve the suitability for clinical work.

V. Conclusions

MELP collimator performed well with ^{123}I, but low resolution makes it unsuitable to use for acquisition of small structures. LEUHR collimators optimized for ^{99m}Tc have highest resolution, but the small difference in septal penetration in favor of LEHR collimator needs to be tested with specific parathyroid phantoms. This study pointed out that thorough testing before clinical application is of high importance in order to understand physical limitations of the imaging process.

Conflict of Interest

The authors declare that they have no conflict of interest.

References

1. Inoue Y, Shirouzu I, Machida T, et al (2003). Physical characteristics of low and medium energy collimators for ^{123}I imaging and simultaneous dual-isotope imaging. Nucl Med Commun, 24(11), 1195-1202.
2. Dobbeleir A, Hambye A, Franken P (1999). Influence of high-energy photons on the spectrum of iodine-123 with low- and medium-energy collimators: consequences for imaging with ^{123}I-labelled compounds in clinical practice. Eur J Nucl Med, 26(6), 655-658.
3. Ivanovic M, Weber D, Loncaric S, et al (1994). Feasibility of dual radionuclide brain imaging with I-123 and Tc-99m. Med Phys, 21(5), 667-674.
4. Madsen M, O'Leary D, Andreasen N, et.al (1993). Dual isotope brain SPECT imaging for monitoring cognitive activation: physical considerations. Nucl Med Commun, 14(5), 391-396.
5. Devous M Sr, Lowe J, & Payne J (1992). Dual-isotope brain SPECT imaging with technetium-99m and iodine-123: validation by phantom studies. J Nucl Med, 33(11), 2030-2035.
6. Neumann D, Obuchowski N, & Difilippo F. (2008). Preoperative ^{123}I/^{99m}Tc-Sestamibi Subtraction SPECT and SPECT/CT in Primary Hyperparathyroidism. J Nucl Med, 49(12), 2012-2017.
7. Neumann D, Esselstyn C Jr, Go R, et al (1997). Comparison of double-phase ^{99m}Tc-sestamibi with ^{123}I-^{99m}Tc-sestamibi subtrac-

tion SPECT in hyperparathyroidism. AJR Am J Roentgenol, 169(6), 1671-1674
8. Ogasawara K, Hashimoto J, Ogawa K, et al (1998). Simultaneous acquisition of iodine-123 emission and technetium-99m transmission data for quantitative brain single-photon emission tomographic imaging. Eur J Nucl Med, 25(11), 1537-1544.
9. Shcherbinin S, Chamoiseau S, & Celler A (2012). Quantitative image reconstruction for dual-isotope parathyroid SPECT/CT: phantom experiments and sample patient studies. Phys Med Biol, 57(15), 4755-4769.
10. NEMA National Electrical Manufacturers Association, NEMA Standards Publication NU 1 (2007): Performance measurements of scintillation cameras.NEMA, Rosslyn, VA
11. Hindie E, Ugur O, Fuster D, et al (2009). 2009 EANM parathyroid guidelines. Eur J Nucl Med Mol Imaging; 36:1201-1216.

Author: Virpi Tunninen, chief physicist
Institute: Satakunta Central Hospital,
Department of Nuclear Medicine
Street: Sairaalantie 3
City: 28500 Pori
Country: Finland
Email: Virpi.tunninen@satshp.fi